Journal of Bioscience and Bioengineering
VOL. 128 No. 4, 424–428, 2019

www.elsevier.com/locate/jbiosc

Time-resolved analysis of short term metabolic adaptation at dark transition in *Synechocystis* sp. PCC 6803

Masaharu Maruyama, Hiroki Nishiguchi, Masakazu Toyoshima, Nobuyuki Okahashi, Fumio Matsuda,* and Hiroshi Shimizu

Department of Bioinformatics Engineering, Graduate School of Information Science and Technology, Osaka University, 1-5 Yamadaoka, Suita, Osaka 565-0871, Japan

Received 13 February 2019; accepted 25 March 2019
Available online 10 April 2019

In photosynthetic organisms, such as cyanobacteria, ATP and NADPH are generated through the light reaction, and then are used for CO_2 fixation in the dark reaction. As light intensity always fluctuates under natural conditions, balancing the cofactor regeneration and consumption is essential to maintain active CO_2 fixation as well as for metabolic engineering of strains that produce biochemicals. In this study, a time-resolved metabolome analysis of *Synechocystis* sp. PCC 6803 (PCC6803) was conducted to investigate a metabolic adaptation at 0–15 min after a sudden shift from light to dark conditions. Rapid accumulation of sedoheptulose 7-phosphate, ribulose 5-phosphate, xylulose 5-phosphate, and 6-phosphogluconate suggested that the central metabolism of PCC6803 was regulated by inactivation of phosphoribulokinase and activation of glucose-6-phosphate dehydrogenase (G6PDH) probably via the redox regulation. The culture and metabolic profile of the Δzwf strain lacking G6PDH showed that the role of G6PDH in regeneration of NADPH could be complemented by the activation of isocitrate dehydrogenase in the TCA cycle, indicating the importance of the rapid regulation of NADPH regeneration after the shift to dark conditions. The mechanism underlying metabolic regulation is also useful for metabolic engineering of PCC6803, as the Δzwf strain produced higher amount of organic acids than wild type.

[**Key words:** *Synechocystis* sp. PCC 6803; Light/dark conditions; Glucose 6-phosphate dehydrogenase; Metabolic adaptation; Metabolome analysis]

Cyanobacteria has proved a promising host for metabolic engineering for the production of various biochemicals from CO_2 via photosynthesis (1–6). A characteristic of cyanobacteria metabolism is that ATP and NADPH are generated through the light reaction, and then are mostly consumed for CO_2 fixation in the dark reaction. As light intensity always fluctuates under natural conditions, the ATP and NADPH regeneration rates by the light reaction should dynamically change in a time-dependent manner. Thus, the dark reaction has a regulatory mechanism that is responsible for maintaining a balance between the regeneration and consumption of ATP and NADPH (7). For instance, activities of some enzymes in the dark reaction are controlled by oxidation and reduction of thiols in the protein via redox regulation (8–10). Furthermore, it has been reported that dynamic metabolic adaptation toward the dark condition, such as inactivation of phosphoribulokinase (PRK) and glyceraldehyde-3-phosphate dehydrogenase (GAPDH) by the formation of CP12/PRK/GAPDH complex, is also redox regulated (11,12). However, the detailed mechanism or process underlying dynamic metabolic adaptation remains unclear.

In this study, a time-resolved metabolome analysis of *Synechocystis* sp. PCC 6803 (PCC6803) was conducted to investigate the mechanism of metabolic regulation in the range at 0–15 min after a sudden shift from light to dark conditions. Rapid accumulation of sedoheptulose 7-phosphate (S7P), ribulose 5-phosphate (Ru5P), xylulose 5-phosphate (Xu5P), and 6-phosphogluconate (6PG) suggested that the central metabolism of PCC6803 was controlled by the inactivation and activation of both PRK and G6PDH, which probably causes decrease and increase in the consumption and regeneration rates of NADPH, respectively. The analysis of gene deletion strain, which lacks G6PDH, indicated that the activation of the TCA cycle was a back-up mechanism for NADPH compensation. The organic acid production by Δzwf strain was greater than that by the wild type, indicating that the mechanism underlying metabolic regulation may also prove useful in the metabolic engineering of PCC6803.

MATERIALS AND METHODS

Strains and culture The *Synechocystis* sp. PCC 6803 glucose-tolerant (GT) strain and *zwf* deletion mutant strain (*zwf*::Km^r (*zwf* (*slr1843*), glucose 6-phosphate dehydrogenase; Km^r kanamycin resistance gene), Δzwf) generated previously (13) were used in this study. Cells were cultured in modified BG-11 medium [2.7 μM EDTA disodium salt, 46 μM H_3BO_3, 20 mM HEPES, 1.6 μM $Na_2MoO_4 \cdot 2H_2O$, 220 μM K_2HPO_4, 300 μM $MgSO_4 \cdot 7H_2O$, 260 μM $CaCl_2$, 9.1 μM $MnCl_2 \cdot 4H_2O$, 0.77 μM $ZnSO_4 \cdot 7H_2O$, 0.32 μM $CuSO_4 \cdot 5H_2O$, 0.17 μM $Co(NO_3)_2 \cdot 6H_2O$, 16 μM $FeCl_2 \cdot 4H_2O$], which was adjusted to a pH of 7.5 using 1 M KOH. Kanamycin (10 μg mL^{-1}) was added to cultures of the Δzwf strain. Cyanobacterial strains were pre-cultured for 4 days in 100 mL flasks with 20 mL of modified BG-11 medium supplemented with 100 mM $NaHCO_3$ at 30 °C with

* Corresponding author. Tel.: +81 6 6879 7433.
E-mail addresses: masaharu_maruyama@ist.osaka-u.ac.jp (M. Maruyama), hiroki_nishiguchi@bio.eng.osaka-u.ac.jp (H. Nishiguchi), toyoshima104@ist.osaka-u.ac.jp (M. Toyoshima), n-okahashi@ist.osaka-u.ac.jp (N. Okahashi), fmatsuda@ist.osaka-u.ac.jp (F. Matsuda), shimizu@ist.osaka-u.ac.jp (H. Shimizu).

1389-1723/$ – see front matter
https://doi.org/10.1016/j.jbiosc.2019.03.016

rotation at 150 rpm under continuous white light illumination with intensity of 40 μmol m^{-2} s^{-1} provided by white light-emitting diodes (LC-LED450W, Taitec, Saitama, Japan). For main culture, this starter culture was inoculated to achieve an optical density of 0.03 at 730 nm (OD_{730}) in 100 mL modified BG-11 medium supplemented with 100 mM $NaHCO_3$, and the culture was incubated at 34 °C with rotation at 150 rpm (BR-43FL, Taitec). For the light/dark experiments, cultures were incubated under alternating 12 h light/12 h dark conditions with the same light intensity during light periods. Cell concentrations in culture were measured by evaluation of optical density at 730 nm (OD_{730}) using a spectrophotometer (UVmini-1240, Shimadzu, Kyoto, Japan).

Metabolome analysis Following the collection of cells [cell density (OD_{730}) × culture volume (mL) = 10], the medium was immediately removed by vacuum filtration using a 0.5-μm pore size filter (PTFE-type membrane, Advantec, Tokyo, Japan), and the cells were soaked in 1.6 mL of pre-cooled methanol. For the dark condition, cells were collected from the flask covered with the aluminum foil under a dim light condition. Cells were then stored at −80 °C until further analysis. Metabolome analysis was performed by the previously described methods (14). The ion-pairing liquid chromatography-tandem mass spectrometry (LC-MS/MS) method (LC: Agilent 1100 series; Agilent Technologies, Santa Clara, CA, USA; MS/MS: API 3200; AB Sciex, Framingham, MA, USA) was employed for the measurement of AcCoA, sugar phosphates (glucose-6-phosphate (G6P), fructose 6-phosphate (F6P), glucose-1-phosphate (G1P), fructose 1,6-bisphosphate (FBP), dihydroxyacetone phosphate (DHAP), erythrose 4-phosphate (E4P), phosphoenolpyruvate (PEP), 6-phosphogluconate (6PG), ribose 5-phosphate (R5P), xylulose 5-phosphate (Xu5P), ribulose 5-phosphate (Ru5P), ribulose 1,5-bisphosphate (RuBP), and sedoheptulose 7-phosphatase (S7P)), and cofactors (AMP, ADP, ATP, NAD^+, and $NADP^+$) (14). For the analysis of organic acids (3-phosphoglycerate (3PG), 2-phosphoglycerate (2PG), pyruvate (Pyr), citrate (Cit), isocitrate (Isocit), α-ketoglutarate (aKG), succinate (Suc), fumaric acid (Fum), and Malic acid (Mal), dried extracts were derivatized by methoxyamine and hydrochloride in pyridine and *N*-methyl-*N*-trimethylsilyltrifluoroacetamide (MSTFA) plus 1% trimethylchlorosilane (TMCS) (Thermo Fisher Scientific, Waltham, MA, USA), and then, analyzed by the gas chromatograph-quadrupole-mass spectrometer (GC-Q-MS) method (GCMSQP-2010 system, Shimadzu) (15). For the analysis of medium, freeze-dried supernatants were dissolved in 50 μL of 40 mg/mL methoxyamine hydrochloride in pyridine and incubated at 30 °C for 1 h. Finally, 50 μL of *N*-methyl-*N*-(*tert*-butyldimethylsilyl)trifluoroacetamide (MTBSTFA) plus 1% tertbutyldimetheylchlorosilane (TBDMS) (Thermo Fisher Scientific) was added and the mixture was incubated at 60 °C for 1 h. The derivatives (1 μL) were analyzed using GC-Q-MS method.

RNA isolation and quantitative real-time PCR Cells were grown in 100 mL of modified BG-11 medium for 7 days under alternating 12 h light/12 h dark conditions. At the transition to dark condition, 5 mL of cyanobacterial culture was collected by centrifugation at 12,000 ×*g* for 1 min. Total RNA was extracted using the NucleoSpin RNA (Macherey-Nagel, Düren, Germany) according to the manufacturer's protocol. The cDNAs were synthesized using the PrimeScript RT reagent Kit (Takara Bio, Kusatsu, Japan) with 3 μg total RNAs. Quantitative real-time PCR was performed using the TB Green Premix Ex Taq II (Takara Bio) according to the manufacturer's instructions, using forward and reverse primers of icd (fw:5′-CCCCGGCTCTGTGATCCT-3′, rev: 5′-TGCCAGCCCATAAATTCCA-3′) and ppc (fw: 5′-CCACCACCACAGCCCTACTAA-3′, rev: 5′-GTCGGAATAGCCCACCATAATTT-3′). The expression level of rnpB (encoding RNaseP subunit B) was used as an internal standard as previously described (16).

RESULTS

The culture profile of *Synechocystis* sp. PCC 6803 under the light/dark condition The cells of *Synechocystis* sp. PCC 6803 GT strain were cultured in a flask under the reciprocal light (12 h)/dark (12 h) condition. During the light period, PCC6803 was grown under the photoautotrophic condition in the BG-11 medium with white light at approximately 40 μmol m^{-2} s^{-1}. Cell density data were recorded at the end of each dark period. The culture profile data showed that the cell density increased in an exponential manner until day 9 (Fig. 1). The specific cell growth rate was 0.037 h^{-1}, which was approximately half of the specific cell growth rate observed under the continuous light condition (13,17,18).

Rapid perturbation of metabolic profile after the sudden shift from light to dark condition The cell sampling was performed at the seventh shift from light to dark condition (at 156 h after the initiation of cultivation), since the cell density reached ca OD_{720} = 1.0. The cells were collected at 0, 1, 2, 3, 5, 7, 10, and 15 min after the shift to dark condition. The sampling at 0 min was done just before the shift to dark phase. The intracellular metabolites were extracted from the cells, and then, subjected to metabolome analysis using LC-MS/MS and GC—MS. The relative abundances of 24 metabolites involved in the central metabolism of PCC6803 were successfully determined in this study (Table S1).

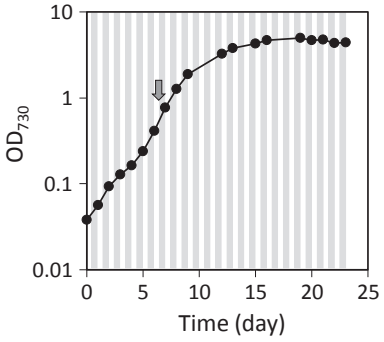

FIG. 1. The culture profile of *Synechocystis* sp. PCC 6803 under light/dark conditions. The cells were cultured in the BG-11 medium under the reciprocal light (12 h, white) and dark (12 h, gray) conditions. Light intensity was approximately 40 μmol m^{-2} s^{-1}. The gray arrow indicates a light to dark shift for sample collections. Values represent mean ± SD of triplicate cultivations.

Fig. 2 is a heat map representation of metabolic abundances relative to 0 min. Levels of ATP, ADP, AMP, and $NADP^+$ tended to be constant during 0—15 min, although the regeneration of ATP and NADPH by the light reaction was stopped by the shift to dark phase. NADPH level was not determined in this study, since its levels were less than the minimum detectable limit. The results suggested that ATP and NADPH turnovers were balanced by inactivation of their consumption pathways and/or activation of alternative regeneration pathways.

The metabolic profile data also revealed that levels of S7P, Ru5P, and Xu5P started to increase at 1 min after the shift to the dark condition. For instance, the levels of S7P at 4 min and 15 min were 10.7- and 5.7-folds larger than that at 0 min (Fig. 2). These results suggested that PRK reaction was rapidly inactivated after the shift to dark phase because only the upstream metabolites of the PRK reaction were accumulated. It has been previously reported that enzymes in the Calvin—Benson cycle of PCC6803, such as GAPDH, fructose 1,6-bisphosphatase, sedoheptulose 1,7-bisphosphatase, and PRK, were dynamically controlled by the thioredoxin-dependent redox regulation (8—10). Another target protein of the redox regulation is CP12, that forms the CP12/PRK/GAPDH protein complex to downregulate the PRK and GAPDH reactions under the dark condition (11,12).

The downstream metabolic pathways of PRK, including ribulose 1,5-bisphosphate carboxylase/oxygenase (RuBisCo), phosphoglycerate kinase (PGK), and GAPDH reactions, compose a carbon fixation pathway which consumes ATP and NADPH. The abundances of the intermediates of this pathway, RuBP and 3PG, at 4 min were 0.45- and 0.62-folds relative to that at 0 min, respectively (Fig. 2). Moreover, levels of other intermediates in the Calvin-Benson cycle tended to decrease after the shift to dark condition, and then, returned to the levels observed at 0 min. These results indicated that the inactivation of PRK played a more important role in the metabolic response against the sudden shift to dark phase. The inactivation of carbon fixation pathway could contribute to keep ATP and NAPDH levels after the shift from light to dark condition.

Among the evaluated metabolites, marked accumulation was observed for 6PG. The level of 6PG increased 8.0-folds at 3 min after the shift to dark phase. 6PG is an intermediate of the oxidative pentose phosphate pathway (oxPPP), synthesized from G6P catalyzed by G6P dehydrogenase (G6PDH) with reproducing NADPH. It has been previously reported that the metabolic flux of the oxPPP

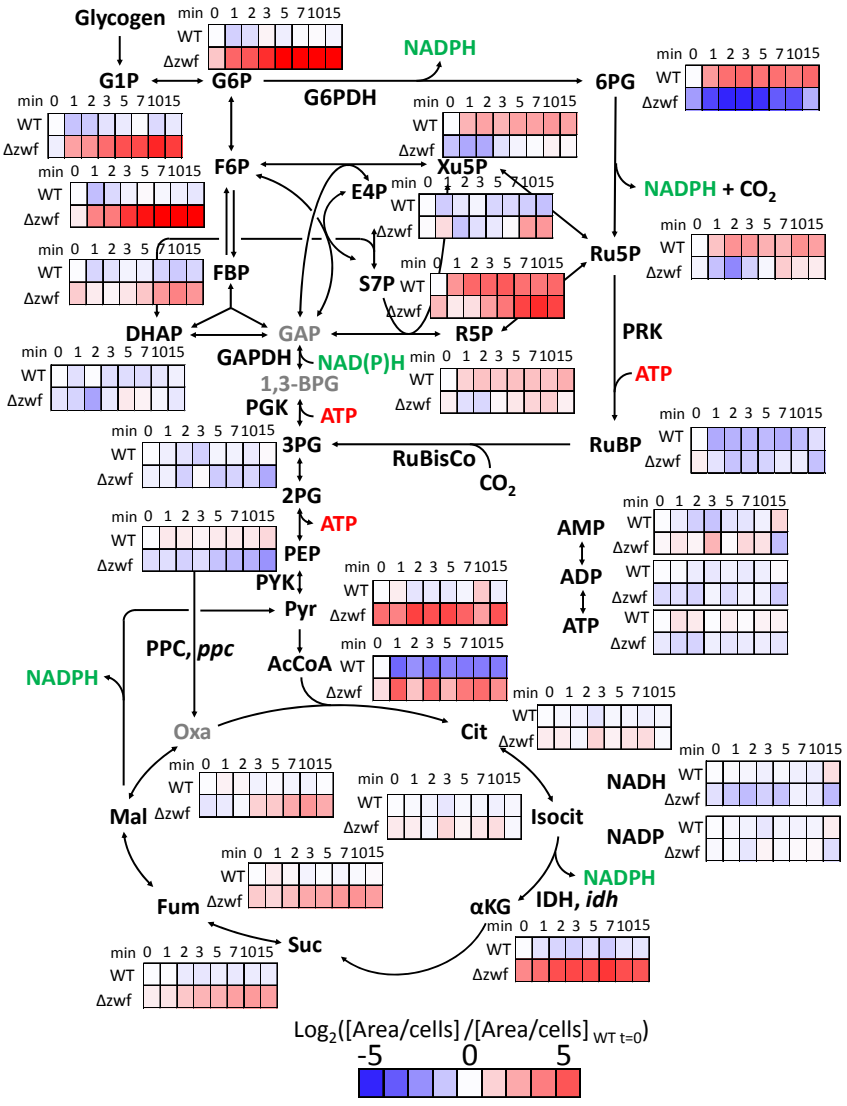

FIG. 2. Metabolic profiles of 24 metabolites involved in the central metabolism of *Synechocystis* sp. PCC 6803 after the shift to dark conditions. Data obtained from the wild type (WT) and Δzwf strains (lacking G6PDH) is shown here. The cells were collected at 0, 1, 2, 3, 5, 7, 10, and 15 min after the seventh shift from light to dark conditions (168 h after the initiation of cultivation). Metabolite abundance relative to that in wild type at 0 min is shown in a heat map representation in the metabolic network. Values represent mean of triplicate cultivations. Abbreviations. 2PG; 2-phosphoglycerate, 3PG; 3-phosphoglycerate, 6PG; 6-phosphogluconate, AcCoA; acetyl coenzyme A, aKG; α-ketoglutarate, Cit; citrate, DHAP; dihydroxyacetone phosphate, E4P; erythrose 4-phosphate, F6P; fructose 6-phosphate, FBP; fructose 1,6-bisphosphate, Fum; fumaric acid, G6P; glucose-6-phosphate, G6PDH; glucose-6-phosphate dehydrogenase, GAP; glyceraldehyde 3-phosphate, GAPDH; glyceraldehyde 3-phosphate dehydrogenase, IDH; isocitrate dehydrogenase, Isocit; isocitrate, Mal; malate, NADP(H); nicotinamide adenine dinucleotide phosphate, PEP; phosphoenolpyruvate, PGK; phosphoglycerate kinase, PPC; phosphoenolpyruvate carboxylase, PRK; phosphoribulokinase, PYK; pyruvate kinase, PYR; pyruvate, R5P; ribose 5-phosphate, Ru5P; ribulose 5-phosphate, RuBP; ribulose 1,5-bisphosphate, RuBisCO; ribulose 1,5-bisphosphate carboxylase/oxygenase, S7P; sedoheptulose 7-phosphate, Suc; succinate, Xu5P; xylulose 5-phosphate.

and the activity of G6PDH protein was also upregulated under the dark condition by the redox regulation via an allosteric effector, OpcA (19,20). In the oxPPP, 6PG is converted to Ru5P while producing CO_2 and NADPH. Under the dark condition, glucose was produced by the glycogen degradation in PCC6803 cells, and then, catabolized via the oxPPP to supply NADPH (21). The results suggested that the upregulation of G6PDH activity is crucial in the rapid metabolic adaptation against the shift to dark condition to compensate NADPH regeneration.

Metabolic response of the mutant strain lacking G6PDH The dynamic compensation of NADPH supply seems to be an important function in the PCC6803 metabolism, suggesting the possibility of some alternative mechanisms. In order to find other pathways that are able to compensate NADPH supply, the Δzwf strain, lacking *zwf* gene which encodes for G6PDH, was used (13). The Δzwf and wild type PCC6803 strains were cultured in the identical light/dark condition for 156 h. The culture profiles of these strains were essentially similar to each other, as has been reported in the previous study (Fig. 3) (22). No effect on the cell growth suggested that the function of the oxPPP was compensated by alternative metabolic pathways, at least under the photoautotrophic and dark condition examined in this study (13).

The metabolic response of the Δzwf strain after the shift from light to dark condition was investigated via the metabolome analysis. Cells were collected at the seventh shift from light to dark condition (at 156 h after the initiation of cultivation, Fig. 2). The levels of the product of G6PDH reaction, 6PG, in the Δzwf strain were very low during the analysis without any transient accumulation. On the other hand, the levels of the substrates of G6PDH, G6P and F6P, were already larger than that of wild type at 0 min (Fig. 2). The results indicated that the lack of G6PDH function

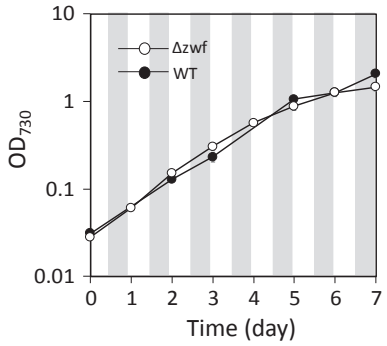

FIG. 3. The culture profile of *Synechocystis* sp. PCC6803 wild type and Δzwf strain (lacking G6PDH) under light/dark conditions. The cells were cultured in the BG-11 medium under the reciprocal light (12 h, white) and dark (12 h, gray) conditions. Light intensity was approximately 40 μmol m^{-2} s^{-1}. Values represent mean ± SD of triplicate cultivations.

affected the cyanobacteria metabolism under the light condition. The levels of G6P and F6P were further increased at 10 min after the shift to dark condition (Fig. 2). These metabolic responses indicated successful knockout of the G6PDH activity.

The metabolic profile data also revealed that the levels of Pyr, AcCoA and the TCA cycle intermediates, such as aKG, Suc, Fum, and Mal were larger than that of wild type at 0 min (Fig. 2). These levels increased after the shift to dark condition in the Δzwf strain (Fig. 2). Interestingly, no increase in Cit and IsoCit levels were observed in the wild type and Δzwf strains. The accumulation pattern of metabolites indicated that pyruvate kinase (PYK) and isocitrate dehydrogenase (IDH) activities should increase rapidly in the Δzwf strains after the shift to dark condition.

In order to confirm the elevation of TCA cycle flux toward the synthesis of Suc, Fum, and Mal, the levels of these organic acids in the culture medium were determined at 168 h. The results showed that the extracellular concentrations of Suc in the wild type and Δzwf cultures were 1.3 ± 0.1 μM and 3.7 ± 0.6 μM, respectively (Fig. 4). Similar accumulation patterns were also observed for other organic acids (Fig. 4). The transcriptional activation of gene expressions was not responsible for the elevation of TCA cycle flux, since expression levels of *ppc* and *idh* genes in Δzwf strain were not higher than those in wild type (Fig. 5).

DISCUSSION

In this study, metabolic profile data were obtained from the *Synechocystis* sp. PCC 6803 cells at 0–15 min after the shift from light to dark conditions. The time-resolved analysis revealed that the levels of upstream metabolites of PRK increased till 1 min (Fig. 2). The rapid response of the Calvin–Benson cycle was consistent with the previous findings, as the PRK and GAPDH reactions were downregulated under the dark condition due to the

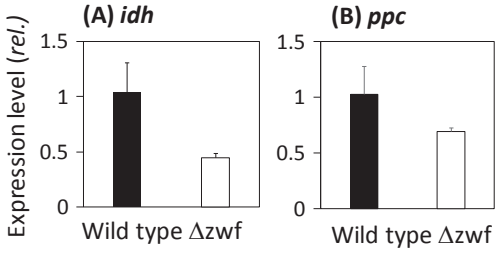

FIG. 5. Expression levels of *idh* and *ppc* genes in *Synechocystis* sp. PCC6803 wild type and Δzwf strains 168 h after the initiation of cultivation. The expression levels of *idh* (A) and *ppc* (B) are shown in the figure. Values represent mean ± SD of three independent experiments. Difference was assessed using a two-sided Student's t-test with an alpha level of 0.05. Asterisk indicates a significant difference ($p < 0.05$).

redox-dependent formation of the CP12/PRK/GAPDH complex (11,12). However, inactivation of GAPDH did not lead to the accumulation of 3PG and RuBP, intermediates in the carbon fixation pathway consisting of PRK, RuBisCo, PGK, and GAPDH reactions. The result suggested that PRK was more responsible for the control of the Calvin–Benson cycle during the shift from light to dark conditions. The rapid inhibition of PRK activity through redox regulation could reduce the levels of ATP and NADPH consumption for carbon-fixation, while ATP and NADPH supply from the photosystems should reduce dramatically after the shift to dark conditions. These results also support that PRK is a major enzyme involved in the regulation of the Calvin–Benson cycle. Metabolic engineering studies have demonstrated that the over-expression of PRK increases the production of ethanol and butanol by cyanobacteria (23,24).

Our analysis also showed a rapid accumulation of 6PG after the shift to dark phase. Since 6PG is a product of G6PDH, which is the first committed enzyme of the oxPPP, the observed metabolic response could be explained by the redox-dependent activation of G6PDH in the dark condition (19). It was expected that the NAPDH supply from the photosystem is depleted a few minutes after the shift to dark condition. On the other hand, G6P is converted from the remaining intermediates of the Calvin-Benson cycle and is supplied by the glycogen degradation (25). Thus, the quick activation of the oxPPP enabled a compensation of NADPH supply to maintain the biosynthesis of cellular components. A drawback of the oxPPP activation, however, was that one molecule of CO_2 had to be taken from a 6PG molecule.

The culture and metabolic profile data of the Δzwf strain indicated that the function of the oxPPP could be complemented by the other metabolic pathway in the PCC6803, since the growth of Δzwf strain cells was essentially identical with that of wild type (Fig. 3). The metabolome analysis of Δzwf strain revealed that the NADPH compensation could be complemented by the activation of IDH in the TCA cycle after the shift to dark condition (Fig. 2). Indeed, the proteome-wide study showed that the redox-dependent control was also found for IDH (10). The metabolic profile data showed that,

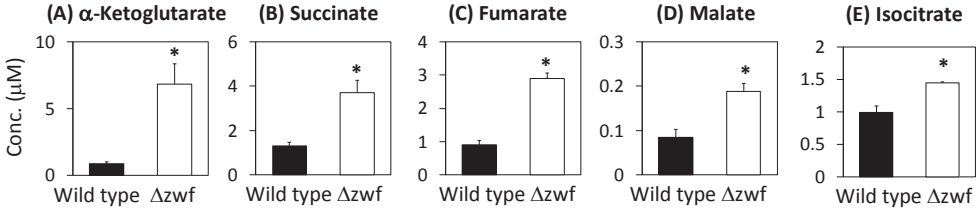

FIG. 4. The concentration of organic acids in the culture medium of *Synechocystis* sp. PCC6803 wild type and Δzwf strain 168 h after the initiation of cultivation. The concentrations of α-ketoglutarate (A), succinate (B), fumarate (C), malate (D), and isocitrate (E) are shown in the figure. Values represent mean ± SD of three independent experiments. Difference was assessed using a two-sided Student's *t*-test with an alpha level of 0.05. Asterisk indicates a significant difference ($p < 0.05$).

since the CO_2 loss by the oxPPP was avoided in Δzwf strain, excess carbons were redirected into the TCA cycle, and then, excreted to the medium (Fig. 4). However, the regulatory mechanism responsible for such metabolic rewiring remains unclear. TCA influx might be increased just because the alternative pathway, G6PDH, is blocked. Moreover, since expression of key enzyme genes, such as *ppc* for the anaplerotic pathway and *idh* for the NAPDH regeneration, was not elevated, some post-transcriptional regulation should be occurring in the Δzwf strain (Fig. 5).

The results of this study suggested that, when cells were suddenly shifted from light to dark condition, the central metabolism of PCC6803 was controlled by the inactivation and activation of PRK and G6PDH activity via redox-regulation. The compensation of NAPDH supply by the oxPPP seems to be vital in PCC6803 metabolism, since the mechanism was backed-up by the activation of the TCA cycle when G6PDH was unavailable. The mechanism of metabolic regulation was also useful for the metabolic engineering of PCC6803 since the organic acid production by Δzwf strain was higher than that by the wild type (Fig. 4). The importance of the oxPPP was also demonstrated in terms of metabolic engineering. For example, the ethanol production by the metabolically engineered PCC6803 was improved by the over-expression of G6PDH under the photoautotrophic condition (26). The deletion of *zwf* gene in *Synechococcus elongatus* PCC 7942 restricted the 2,3-butanediol production under continuous light conditions (24), suggesting that effects of the engineering of the oxPPP on the central metabolism is still unpredictable. The time-resolved metabolome analysis will be useful for further investigation of the role of the oxPPP to elucidate the regulatory mechanisms required for the rational engineering of the cyanobacteria metabolism (27,28).

Supplementary data to this article can be found online at https://doi.org/10.1016/j.jbiosc.2019.03.016.

ACKNOWLEDGMENTS

We thank Prof. Yoshihiro Toya (Osaka University) for helpful comments on this manuscript and for providing technical support. This work was supported, in part, by Grants-in-Aid for Scientific Research (grant numbers 16H06552, 16H06559, and 17H06303).

References

1. **Lai, M. C. and Lan, E. I.:** Advances in metabolic engineering of cyanobacteria for photosynthetic biochemical production, Metabolites, **5**, 636–658 (2015).
2. **Angermayr, S. A., Gorchs Rovira, A., and Hellingwerf, K. J.:** Metabolic engineering of cyanobacteria for the synthesis of commodity products, Trends Biotechnol., **33**, 352–361 (2015).
3. **Oliver, N. J., Rabinovitch-Deere, C. A., Carroll, A. L., Nozzi, N. E., Case, A. E., and Atsumi, S.:** Cyanobacterial metabolic engineering for biofuel and chemical production, Curr. Opin. Chem. Biol., **35**, 43–50 (2016).
4. **Namakoshi, K., Nakajima, T., Yoshikawa, K., Toya, Y., and Shimizu, H.:** Combinatorial deletions of *glgC* and *phaCE* enhance ethanol production in *Synechocystis* sp. PCC 6803, J. Biotechnol., **239**, 13–19 (2016).
5. **Osanai, T., Shirai, T., Iijima, H., Nakaya, Y., Okamoto, M., Kondo, A., and Hirai, M. Y.:** Genetic manipulation of a metabolic enzyme and a transcriptional regulator increasing succinate excretion from unicellular cyanobacterium, Front. Microbiol., **6**, 1064 (2015).
6. **Atsumi, S., Higashide, W., and Liao, J. C.:** Direct photosynthetic recycling of carbon dioxide to isobutyraldehyde, Nat. Biotechnol., **27**, 1177–1180 (2009).
7. **Tamoi, M., Nagaoka, M., Yabuta, Y., and Shigeoka, S.:** Carbon metabolism in the Calvin cycle, Plant Biotechnol. J., **22**, 355–360 (2005).
8. **Ansong, C., Sadler, N. C., Hill, E. A., Lewis, M. P., Zink, E. M., Smith, R. D., Beliaev, A. S., Konopka, A. E., and Wright, A. T.:** Characterization of protein redox dynamics induced during light-to-dark transitions and nutrient limitation in cyanobacteria, Front. Microbiol., **5**, 325 (2014).
9. **Tsukamoto, Y., Fukushima, Y., Hara, S., and Hisabori, T.:** Redox control of the activity of phosphoglycerate kinase in *Synechocystis* sp. PCC6803, Plant Cell Physiol., **54**, 484–491 (2013).
10. **Guo, J., Nguyen, A. Y., Dai, Z., Su, D., Gaffrey, M. J., Moore, R. J., Jacobs, J. M., Monroe, M. E., Smith, R. D., Koppenaal, D. W., Pakrasi, H. B., and Qian, W. J.:** Proteome-wide light/dark modulation of thiol oxidation in cyanobacteria revealed by quantitative site-specific redox proteomics, Mol. Cell. Proteomics, **13**, 3270–3285 (2014).
11. **Wedel, N. and Soll, J.:** Evolutionary conserved light regulation of Calvin cycle activity by NADPH-mediated reversible phosphoribulokinase/CP12/glyceraldehyde-3-phosphate dehydrogenase complex dissociation, Proc. Natl. Acad. Sci. USA, **95**, 9699–9704 (1998).
12. **Tamoi, M., Miyazaki, T., Fukamizo, T., and Shigeoka, S.:** The Calvin cycle in cyanobacteria is regulated by CP12 via the NAD(H)/NADP(H) ratio under light/dark conditions, Plant J., **42**, 504–513 (2005).
13. **Ueda, K., Nakajima, T., Yoshikawa, K., Toya, Y., Matsuda, F., and Shimizu, H.:** Metabolic flux of the oxidative pentose phosphate pathway under low light conditions in *Synechocystis* sp. PCC 6803, J. Biosci. Bioeng., **126**, 38–43 (2018).
14. **Nishino, S., Okahashi, N., Matsuda, F., and Shimizu, H.:** Absolute quantitation of glycolytic intermediates reveals thermodynamic shifts in *Saccharomyces cerevisiae* strains lacking *PFK1* or *ZWF1* genes, J. Biosci. Bioeng., **120**, 280–286 (2015).
15. **Kato, H., Izumi, Y., Hasunuma, T., Matsuda, F., and Kondo, A.:** Widely targeted metabolic profiling analysis of yeast central metabolites, J. Biosci. Bioeng., **113**, 665–673 (2012).
16. **Schlebusch, M. and Forchhammer, K.:** Requirement of the nitrogen starvation-induced protein Sll0783 for polyhydroxybutyrate accumulation in *Synechocystis* sp. strain PCC 6803, Appl. Environ. Microbiol., **76**, 6101–6107 (2010).
17. **Nakajima, T., Kajihata, S., Yoshikawa, K., Matsuda, F., Furusawa, C., Hirasawa, T., and Shimizu, H.:** Integrated metabolic flux and omics analysis of *Synechocystis* sp. PCC 6803 under mixotrophic and photoheterotrophic conditions, Plant Cell Physiol., **55**, 1605–1612 (2014).
18. **Yoshikawa, K., Toya, Y., and Shimizu, H.:** Metabolic engineering of *Synechocystis* sp. PCC 6803 for enhanced ethanol production based on flux balance analysis, Bioproc. Biosyst. Eng., **40**, 791–796 (2017).
19. **Sundaram, S., Karakaya, H., Scanlan, D. J., and Mann, N. H.:** Multiple oligomeric forms of glucose-6-phosphate dehydrogenase in cyanobacteria and the role of OpcA in the assembly process, Microbiology, **144**, 1549–1556 (1998).
20. **Hagen, K. D. and Meeks, J. C.:** The unique cyanobacterial protein OpcA is an allosteric effector of glucose-6-phosphate dehydrogenase in *Nostoc punctiforme* ATCC 29133, J. Biol. Chem., **276**, 11477–11486 (2001).
21. **Wan, N., DeLorenzo, D. M., He, L., You, L., Immethun, C. M., Wang, G., Baidoo, E. E. K., Hollinshead, W., Keasling, J. D., Moon, T. S., and Tang, Y. J.:** Cyanobacterial carbon metabolism: fluxome plasticity and oxygen dependence, Biotechnol. Bioeng., **114**, 1593–1602 (2017).
22. **Jansén, T., Kurian, D., Raksajit, W., York, S., Summers, M. L., and Mäenpää, P.:** Characterization of trophic changes and a functional oxidative pentose phosphate pathway in *Synechocystis* sp. PCC 6803, Acta Physiol. Plant., **32**, 511–518 (2010).
23. **Nishiguchi, H., Hiasa, N., Uebayashi, K., Liao, J., Shimizu, H., and Matsuda, F.:** Transomics data-driven, ensemble kinetic modeling for system-level understanding and engineering of the cyanobacteria central metabolism, Metab. Eng., **52**, 273–283 (2019).
24. **Kanno, M., Carroll, A. L., and Atsumi, S.:** Global metabolic rewiring for improved CO_2 fixation and chemical production in cyanobacteria, Nat. Commun., **8**, 14724 (2017).
25. **Hanai, M., Sato, Y., Miyagi, A., Kawai-Yamada, M., Tanaka, K., Kaneko, Y., Nishiyama, Y., and Hihara, Y.:** The effects of dark incubation on cellular metabolism of the wild type cyanobacterium *Synechocystis* sp. PCC 6803 and a mutant lacking the transcriptional regulator cyAbrB2, Life (Basel), **4**, 770–787 (2014).
26. **Choi, Y. N. and Park, J. M.:** Enhancing biomass and ethanol production by increasing NADPH production in *Synechocystis* sp. PCC 6803, Bioresour. Technol., **213**, 54–57 (2016).
27. **Ito, S. and Osanai, T.:** Single amino acid change in 6-phosphogluconate dehydrogenase from *Synechocystis* conveys higher affinity for $NADP^+$ and altered mode of inhibition by NADPH, Plant Cell Physiol., **59**, 2452–2461 (2018).
28. **Matsuda, F., Toya, Y., and Shimizu, H.:** Learning from quantitative data to understand central carbon metabolism, Biotechnol. Adv., **35**, 971–980 (2017).